Singularity Analysis and Avoidance of Variable-Speed Control Moment Gyros – Part II : Power Constraint Case

Hyungjoo Yoon* and Panagiotis Tsiotras†

Georgia Institute of Technology, Atlanta, Georgia 30332-0150, USA

A Variable Speed Control Moment Gyro (VSCMG) is a relatively recent torque actuator device for spacecraft attitude control. As implied by its name, a VSCMG is a single-gimbal control moment gyro (CMG) with a flywheel having variable speed. Owing to this extra degree of freedom, a VSCMG can be used to achieve additional objectives, such as power tracking and/or singularity avoidance, as well as attitude control. In this article, a singularity analysis and a singularity avoidance method are proposed for the case when a VSCMG cluster is used as part of an integrated power/attitude control system (IPACS) onboard a satellite. The gimbal rates of the VSCMGs are used to provide the reference-tracking torques, while the wheel accelerations are used both for attitude tracking and power reference tracking. The latter is achieved by storing or releasing the kinetic energy stored in the VSCMG flywheels. A null motion method to avoid singularities is also presented and a criterion is developed to determine the momentum region over which this method will successfully avoid singularities. This criterion can be used to size the wheels and develop appropriate momentum damping strategies tailored to specific mission requirements.

I. Introduction

Most spacecraft use chemical batteries to store excess energy generated by the solar panels during the period of exposure to the sun. These batteries are used to provide power for the spacecraft subsystems during the eclipse and are re-charged when the spacecraft is in the sunlight. However, the use of chemical batteries introduces several problems, such as limited life cycle, shallow depth of discharge (approximately 20-30% of their rated energy-storage capacity), large weight and strict temperature limits (at or below 20°C in a low-Earth orbit).

An alternative to chemical batteries is the use of flywheels to store energy. The use of flywheels as "mechanical batteries" has the benefit of increased efficiency (up to 90% depth of discharge with essentially unlimited life), and the ability to operate in a relatively hot (up to 40°C) environment. Most importantly, flywheels offer the potential to combine the energy-storage and the attitude-control functions into a single device, thus increasing reliability and significantly reducing the overall weight and spacecraft size. This implies increased payload capacity and significant reduction of launch and fabrication costs. This concept, termed the Integrated Power and Attitude Control System (IPACS) has been studied since the 1960s, but it has become particularly popular during the last decade. A complete survey of IPACS has been given in Refs. 1 and 2.

Variable Speed Control Moment Gyros (VSCMGs) have been used for attitude control and energy storage for an IPACS in the authors' previous work.[3] The concept of a VSCMG was first introduced by Ford and Hall[4] where it was called "gimballed momentum wheel." The term VSCMG was coined in Ref. 5, emphasizing the fact that these devices typically function as conventional CMGs. Whereas the wheel speed of a conventional CMG is kept constant, the wheel speed of a VSCMG is allowed to vary continuously. A VSCMG can thus

*Graduate Student, School of Aerospace Engineering. Email: hyungjoo_yoon@ae.gatech.edu. Tel: (404) 385-1682. Student Member AIAA.

†Associate Professor, School of Aerospace Engineering. Email: p.tsiotras@ae.gatech.edu. Tel: (404) 894-9526. Fax: (404) 894-2760. Associate Fellow AIAA. Corresponding author.

be considered as a hybrid between a reaction wheel and a conventional CMG. The extra degree of freedom, owing to the wheel speed changes, can be used to avoid singularities. It also allows a VSCMG to be used as an actuator in an Integrated Power/Attitude Control System (IPACS).[1,3] The control algorithm performs both the attitude and power tracking goals simultaneously.

It is well known that a VSCMG cluster can always generate an output torque with arbitrarily commanded direction and magnitude. Moreover, it is also known that a gradient method with null motion can avoid the singular states of VSCMGs. In these singular states the VSCMG cluster requires large control inputs in order to generate the commanded output torque.[6] Yet, if the VSCMG cluster is part of an IPACS with strict power as well as attitude tracking requirements, there exist singular gimbal angle and wheel speed configurations, for which the VSCMGs cannot meet both attitude and power tracking requirements.[3]

In the present article, a singularity avoidance method using single gimbal variable speed control moment gyros (VSCMGs) is presented. It complements the results of Refs. 3 and 7 as well as those of Ref. 8 in several aspects. Whereas Refs. 3 and 7 did not deal with the singularity problem explicitly, the present paper deals specifically with this problem. Moreover, in Ref. 8 the authors restrict the discussion to the case of attitude tracking only, whereas in the present article we include the case of simultaneous attitude and power tracking. As shown in Section III this has several important repercussions to the singularity classification and avoidance problem.

II. System Model and Preliminaries

There are several ways to configure a number of VSCMG units. The standard pyramid configuration with four VSCMG units is emphasized in this article is shown in Fig. 1. The skew angle θ in Fig. 1 is chosen as $\cos\theta = 1/\sqrt{3}$ ($\theta \approx 54.74^\circ$) so that the pyramid becomes half of a regular octahedron. This configuration has been studied extensively because it is only once-redundant and its momentum envelope (see Section II-B) is nearly spherical[9] and three-axis symmetric.[10] The mutually orthogonal unit vectors $\mathbf{g}_i$, $\mathbf{s}_i$ and $\mathbf{t}_i$, $i = 1, \cdots, 4$, are defined as in Refs. 6 and 11.

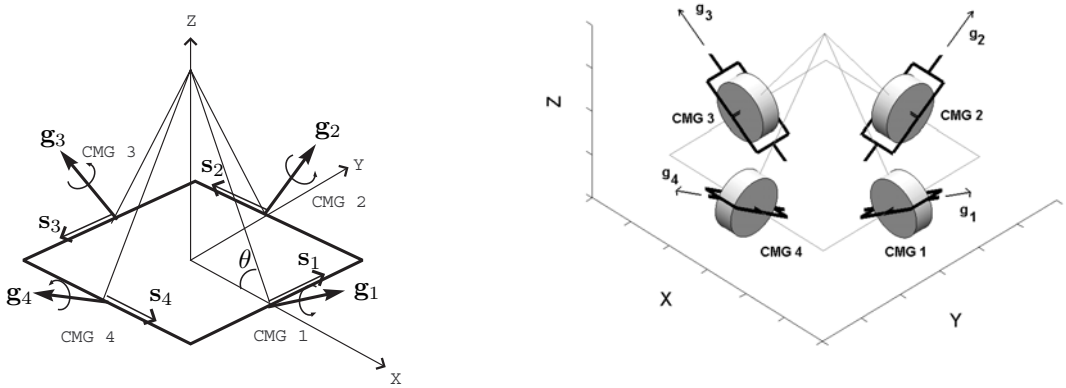

(a) (b)

Figure 1. A VSCMG system with pyramid configuration

The total angular momentum $\mathbf{H}$ of the VSCMG system is the vector sum of the individual momenta of each wheel

$$\mathbf{H}(\gamma_1, \cdots, \gamma_N, \Omega_1, \cdots, \Omega_N) = \sum_{i=1}^{N} h_i \mathbf{s}_i, \tag{1}$$

where $h_i(\Omega_i)$ is the angular momentum of ith wheel. The torque equation becomes

$$\mathbf{T} = \dot{\mathbf{H}} = \sum_{i=1}^{N} h_i \mathbf{t}_i \dot{\gamma}_i + \sum_{i=1}^{N} \mathbf{s}_i I_{\mathrm{ws}_i} \dot{\Omega}_i, \tag{2}$$

and in matrix form,

$$\begin{bmatrix} C(\boldsymbol{\Omega}, \boldsymbol{\gamma}) & D(\boldsymbol{\gamma}) \end{bmatrix} \begin{bmatrix} \dot{\boldsymbol{\gamma}} \\ \dot{\boldsymbol{\Omega}} \end{bmatrix} = \mathbf{T}, \tag{3}$$

where $C : \mathbb{R}^N \times [0, 2\pi)^N \to \mathbb{R}^{3\times N}$ and $D : [0, 2\pi)^N \to \mathbb{R}^{3\times N}$ are matrix-valued functions given by

$$C(\boldsymbol{\Omega}, \boldsymbol{\gamma}) \triangleq [I_{\mathrm{ws}_1} \Omega_1 \mathbf{t}_1, \cdots, I_{\mathrm{ws}_N} \Omega_N \mathbf{t}_N] \tag{4}$$

$$D(\boldsymbol{\gamma}) \triangleq [I_{\mathrm{ws}_1} \mathbf{s}_1, \cdots, I_{\mathrm{ws}_N} \mathbf{s}_N] \tag{5}$$

and where $\boldsymbol{\gamma} \triangleq (\gamma_1, \ldots, \gamma_N)^T \in [0, 2\pi)^N$ and $\boldsymbol{\Omega} \triangleq (\Omega_1, \ldots, \Omega_N)^T \in \mathbb{R}^N$. It is well known that we can always solve Eq. (3) for any given torque command $\mathbf{T}$ with a VSCMG system in the pyramid configuration. Yet, it is desirable to keep $\operatorname{rank} C = 3$. In the sequel we *define* as a "singularity of a VSCMG cluster" the rank deficiency of the matrix C, even though the VSCMGs will be able to generate an arbitrary torque at such cases. See Refs. 6 and 11 for more details.

A. Attitude and Power Tracking Control Law

In Ref. 1, the authors have introduced a control method for the simultaneous attitude and power tracking problem for the case of a rigid spacecraft with N momentum wheels. These results have been extended to the case of N VSCMGs in Refs. 3, 7. By setting the gimbal angles in Ref. 3 to be constant, one can retrieve the results of Ref. 1 as a special case.

The total kinetic energy stored in the wheels of the VSCMG cluster is

$$E \triangleq \tfrac{1}{2} \boldsymbol{\Omega}^T I_{\mathrm{ws}} \boldsymbol{\Omega} \tag{6}$$

where $I_{\mathrm{ws}} \triangleq \operatorname{diag}[I_{\mathrm{ws}_1}, \cdots, I_{\mathrm{ws}_N}] \in \mathbb{R}^{N\times N}$. Hence, the power (rate of change of the energy) is given by

$$\begin{aligned} P = \frac{\mathrm{d}E}{\mathrm{d}t} &= \boldsymbol{\Omega}^T I_{\mathrm{ws}} \dot{\boldsymbol{\Omega}} \\ &= \begin{bmatrix} 0 & \boldsymbol{\Omega}^T I_{\mathrm{ws}} \end{bmatrix} \begin{bmatrix} \dot{\boldsymbol{\gamma}} \\ \dot{\boldsymbol{\Omega}} \end{bmatrix}. \end{aligned} \tag{7}$$

This equation is augmented to the attitude tracking equation (3), to obtain

$$Q_p \mathbf{u} = \mathbf{L} \tag{8}$$

where

$$\mathbf{u} \triangleq \begin{bmatrix} \dot{\boldsymbol{\gamma}} \\ \dot{\boldsymbol{\Omega}} \end{bmatrix}, \qquad Q_p \triangleq \begin{bmatrix} C(\boldsymbol{\Omega}, \boldsymbol{\gamma}) & D(\boldsymbol{\gamma}) \\ \mathbf{0}_{1\times N} & \boldsymbol{\Omega}^T I_{\mathrm{ws}} \end{bmatrix}, \qquad \mathbf{L} \triangleq \begin{bmatrix} \mathbf{T} \\ P \end{bmatrix}.$$

The existence of a solution to Eq. (8) depends on the rank of the coefficient matrix $Q_p \in \mathbb{R}^{4\times 2N}$. If $\operatorname{rank} Q_p = 4$, then Eq. (8) always has a solution, for example,

$$\begin{bmatrix} \dot{\boldsymbol{\gamma}} \\ \dot{\boldsymbol{\Omega}} \end{bmatrix} = W Q_p^T (Q_p W Q_p^T)^{-1} \mathbf{L}, \tag{9}$$

for some $2N \times 2N$ weighting matrix W. However, if $\operatorname{rank} Q_p = 3$, it is not possible to solve equation (8)*. In Ref. 3 the authors have shown that a sufficient (but not necessary) condition for $\operatorname{rank} Q_p = 4$ is that $\operatorname{rank} C = 3$. This means that the issue of singularity avoidance for a VSCMG system (in terms of the rank deficiency of C) becomes more pronounced in case of a power tracking requirement.

*Notice that rank $Q_p \geq 3$, since rank $[C(\boldsymbol{\Omega}, \boldsymbol{\gamma})\ D(\boldsymbol{\gamma})] = 3$ for all $\boldsymbol{\Omega} \in \mathbb{R}^N$ and $\boldsymbol{\gamma} \in [0, 2\pi)^N$.

B. Brief Review of the Singularities of a CMG system

Before continuing with the analysis of the singularities of VSCMGs, it is imperative to briefly review the singularities of the conventional CMGs. This will also allow the introduction of the key terminology which is essential in the ensuing analysis of VSCMGs.

For simplicity, and without loss of generality, let us assume that $h_i = 1$ for $i = 1, \cdots, N$. Then the torque equation (3) becomes

$$C(\boldsymbol{\gamma})\, \dot{\boldsymbol{\gamma}} = \mathbf{T} \tag{10}$$

where $C(\boldsymbol{\gamma}) = [\mathbf{t}_1, \cdots, \mathbf{t}_N]$. In order to generate a torque $\mathbf{T}$ along an arbitrary direction, we need rank $C(\boldsymbol{\gamma})$ $= 3$ for all $\boldsymbol{\gamma} \in [0, 2\pi)^N$. If rank $C(\boldsymbol{\gamma}_s) \neq 3$ for some $\boldsymbol{\gamma}_s$, however, $\dot{\boldsymbol{\gamma}}$ cannot be calculated for arbitrary torque commands.[†] Thus, henceforth we define the singularities of a CMG system as the gimbal states $\boldsymbol{\gamma}_s$ for which rank $C(\boldsymbol{\gamma}_s) = 2$.[‡] In the singular states all unit vectors $\mathbf{t}_i$ lie on the same plane, and we can thus define a singular direction vector $\mathbf{u}$ which is normal to this plane. That is,

$$\mathbf{u}^T \mathbf{t}_i = 0, \quad \forall\, i = 1, \cdots, N. \tag{11}$$

Moreover, $\mathbf{t}_i$ is normal to $\mathbf{g}_i$ by definition, so $\mathbf{t}_i$ is normal to the plane spanned by $\mathbf{g}_i$ and $\mathbf{u}$. Geometrically this means that each $\mathbf{s}_i$ has a maximal or minimal (negatively maximal) projection onto the singular vector $\mathbf{u}$, i.e., the dot product $\mathbf{u} \cdot \mathbf{s}_i$ is maximal or minimal,[13] as shown in Fig. 2.

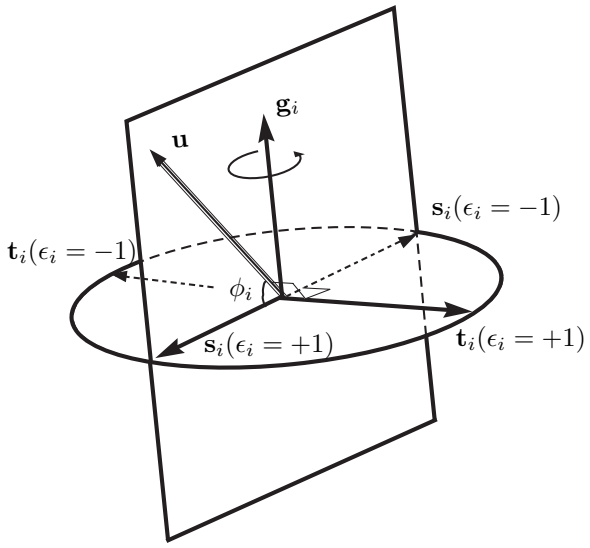

Figure 2. Vectors at a singular gimbal state

For a given singular vector $\mathbf{u} \neq \pm\mathbf{g}_i$, there are two possibilities:

$$\mathbf{u} \cdot \mathbf{t}_i = 0 \text{ and } \mathbf{u} \cdot \mathbf{s}_i > 0, \quad \text{or} \quad \mathbf{u} \cdot \mathbf{t}_i = 0 \text{ and } \mathbf{u} \cdot \mathbf{s}_i < 0. \tag{12}$$

Defining $\epsilon_i \triangleq \text{sign}(\mathbf{u} \cdot \mathbf{s}_i)$, the torque axis vector and the spin axis vector at a singular state can be obtained as

$$\mathbf{t}_i = \epsilon_i\, \mathbf{g}_i \times \mathbf{u} / |\mathbf{g}_i \times \mathbf{u}|, \quad \mathbf{u} \neq \pm\mathbf{g}_i, \quad i = 1, \cdots, N \tag{13}$$

$$\mathbf{s}_i = \mathbf{t}_i \times \mathbf{g}_i = \epsilon_i\, (\mathbf{g}_i \times \mathbf{u}) \times \mathbf{g}_i / \|\mathbf{g}_i \times \mathbf{u}\|, \quad \mathbf{u} \neq \pm\mathbf{g}_i, \quad i = 1, \cdots, N \tag{14}$$

and therefore the total angular momentum at the singular states corresponding to a singular direction $\mathbf{u}$ is expressed as[12–14]

$$\mathbf{H} = \sum_{i=1}^{N} \mathbf{s}_i = \sum_{i=1}^{N} \epsilon_i\, (\mathbf{g}_i \times \mathbf{u}) \times \mathbf{g}_i / \|\mathbf{g}_i \times \mathbf{u}\|, \quad \mathbf{u} \neq \pm\mathbf{g}_i. \tag{15}$$

[†]Even in this case, there may exist a solution $\dot{\boldsymbol{\gamma}}$ to (10), if the required torque $\mathbf{T}$ lies in the two-dimensional range of $C(\boldsymbol{\gamma}_s)$, but this can be treated as an exceptional case.

[‡]Rank $C = 1$ can happen only in very special configuration, for example, in roof-type configuration,[12] so we neglect this case.

Hence, given a set of ϵ_i's, we can draw a singular surface, which is defined as the locus of the total momentum vector at the singular states, for all $\mathbf{u} \in \mathbb{R}^3$ with $\|\mathbf{u}\| = 1, \mathbf{u} \neq \pm\mathbf{g}_i$ where $\|\cdot\|$ denotes the Euclidian norm. Figure 3 shows examples of these singular surfaces for a pyramid configuration for two different combinations of $\epsilon_1, \epsilon_2, \epsilon_3, \epsilon_4$.

Among the singular surfaces of a CMG system, of a special interest is the angular momentum envelope, which is defined as the boundary of the maximum workspace of the total angular momentum $\mathbf{H}$. The angular momentum envelope of a CMG cluster in a pyramid configuration consists of two types of singular surfaces which are connected to each other smoothly. The first type corresponds to the case when all ϵ_i are positive, i.e., the angular momentum of each CMG unit has a maximal projection onto the singular direction[§] as shown in Fig. 3(a). Notice that this singular surface does not cover the whole momentum envelope, and there exist

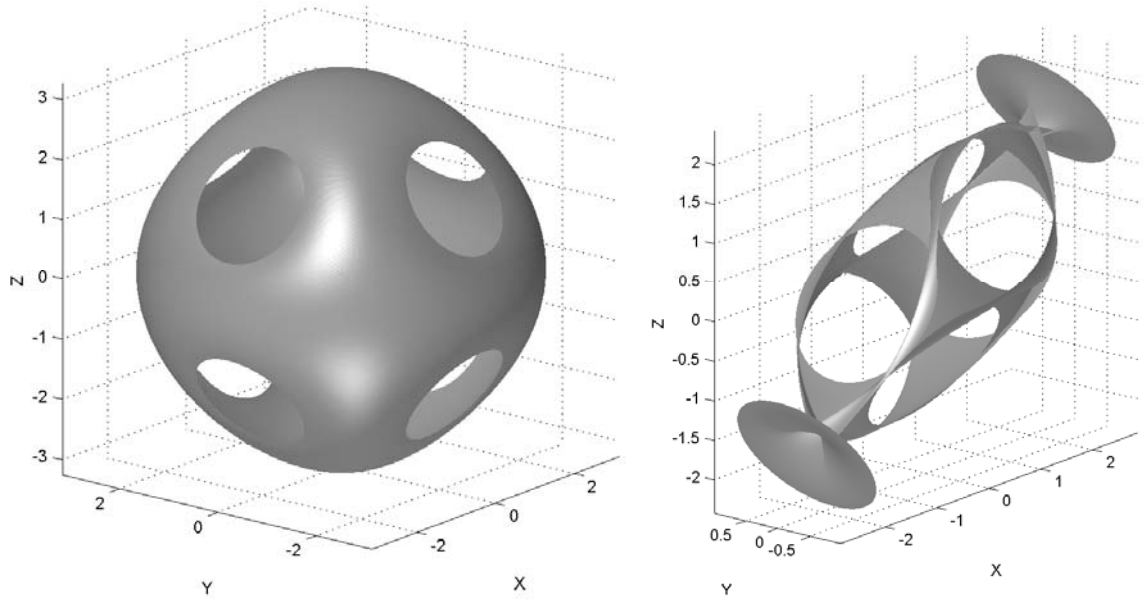

Figure 3. Singular surfaces of CMGs in pyramid configuration a) $\epsilon_1 = \epsilon_2 = \epsilon_3 = \epsilon_4 = +1$**, b)** $\epsilon_1 = -1$**,** $\epsilon_2 = \epsilon_3 = \epsilon_4 = +1$

holes on the surface. These holes are smoothly connected to the second type of the singular surface, for which one and only one of the ϵ_i, $i \in \{1, \cdots, N\}$ is negative (or only one positive due to symmetry).[12,13] This singular surface produces a trumpet-like funnel at the holes which completes the envelope and is shown in Fig. 3(b).

In conclusion, the complete momentum envelope is composed of the singular surface with $\epsilon_i > 0$ for $i = 1, \cdots, N$ and the external portion of the singular surface with one and only one negative ϵ_i. Figure 4 shows the complete angular momentum envelop with a cut revealing part of the rather complicated internal singular surface.

III. Singularity Analysis of VSCMGs With Power Tracking

In order to investigate the existence of null motion for the case of both attitude and power tracking, we first notice that in this case the following conditions must be true

$$C(\mathbf{\Omega}(t), \boldsymbol{\gamma}(t))\dot{\boldsymbol{\gamma}}(t) + D(\boldsymbol{\gamma}(t))\dot{\mathbf{\Omega}}(t) = 0, \quad \text{at time } t \tag{16}$$

$$C(\mathbf{\Omega}(t + \mathrm{d}t), \boldsymbol{\gamma}(t + \mathrm{d}t))\dot{\boldsymbol{\gamma}}(t + \mathrm{d}t) + D(\boldsymbol{\gamma}(t + \mathrm{d}t))\dot{\mathbf{\Omega}}(t + \mathrm{d}t) = 0, \quad \text{at time } t + \mathrm{d}t \tag{17}$$

[§]The case of all negative ϵ_i is also on the angular momentum envelope due to symmetry.

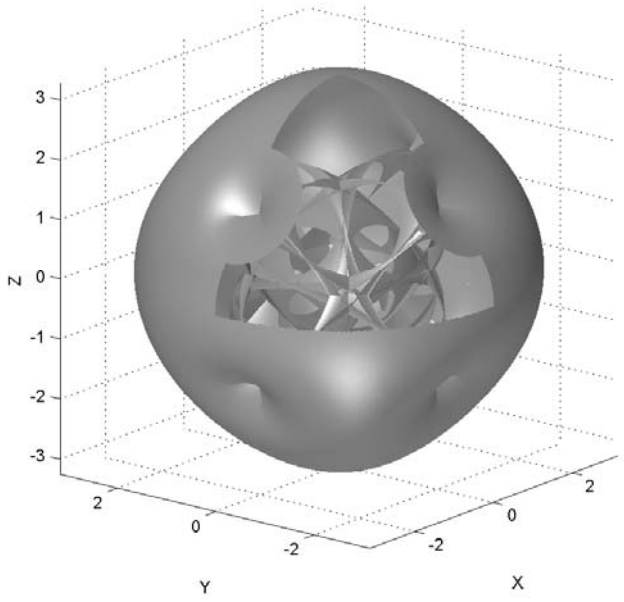

Figure 4. Angular momentum envelope of CMGs

and

$$\boldsymbol{\Omega}^T(t) I_{\rm ws} \dot{\boldsymbol{\Omega}}(t) = 0, \quad \text{at time } t \tag{18}$$

$$\boldsymbol{\Omega}^T(t+\mathrm{d}t) I_{\rm ws} \dot{\boldsymbol{\Omega}}(t+\mathrm{d}t) = 0, \quad \text{at time } t+\mathrm{d}t \tag{19}$$

where $C(\boldsymbol{\Omega}, \boldsymbol{\gamma})$ and $D(\boldsymbol{\gamma})$ as in (4)-(5). In a similar fashion as in Ref. 6, these conditions lead to the condition that a null motion exists if and only if there exist $\ddot{\boldsymbol{\gamma}}(t) \in \mathbb{R}^N$ and $\ddot{\boldsymbol{\Omega}}(t) \in \mathbb{R}^N$ such that

$$\left[\begin{array}{cc} C(\boldsymbol{\Omega}(t), \boldsymbol{\gamma}(t)) & D(\boldsymbol{\gamma}(t)) \\ \mathbf{0}_{1\times N} & \boldsymbol{\Omega}^T(t) I_{\rm ws} \end{array} \right] \left[\begin{array}{c} \ddot{\boldsymbol{\gamma}}(t) \\ \ddot{\boldsymbol{\Omega}}(t) \end{array} \right] = \left[\begin{array}{c} \boldsymbol{\zeta}_1 \\ \zeta_2 \end{array} \right], \tag{20}$$

where $\boldsymbol{\zeta}_1 \in \mathbb{R}^3$ and $\zeta \in \mathbb{R}$ from

$$\boldsymbol{\zeta}_1 \triangleq -2 \sum_{i=1}^{N} I_{{\rm ws}i} \mathbf{t}_i \dot{\gamma}_i \dot{\Omega}_i + \sum_{i=1}^{N} I_{{\rm ws}i} \Omega_i \mathbf{s}_i \dot{\gamma}_i^2, \tag{21}$$

$$\zeta_2 \triangleq -\dot{\boldsymbol{\Omega}}^T I_{\rm ws} \dot{\boldsymbol{\Omega}} = -\sum_{i=1}^{N} I_{{\rm ws}_i} \dot{\Omega}_i^2. \tag{22}$$

Next, we show that a solution to (20) exists if and only if rank $M = 2$, where

$$M \triangleq \left[\begin{array}{cccc} I_{{\rm ws}_1} \mathbf{u}^T \mathbf{s}_1 & I_{{\rm ws}_2} \mathbf{u}^T \mathbf{s}_2 & \cdots & I_{{\rm ws}_N} \mathbf{u}^T \mathbf{s}_N \\ I_{{\rm ws}_1} \Omega_1 & I_{{\rm ws}_2} \Omega_2 & \cdots & I_{{\rm ws}_N} \Omega_N \end{array} \right]. \tag{23}$$

To this end, notice that a solution to (20) exists if and only if $\boldsymbol{\zeta} \triangleq [\boldsymbol{\zeta}_1^T \ \zeta_2]^T \in \mathcal{R}[Q_p]$, equivalently, if and only if $\mathbf{v}^T \boldsymbol{\zeta} = 0$ for all nonzero $\mathbf{v} \in \mathcal{R}^{\perp}[Q_p]$. Notice that

$$\mathcal{R}^{\perp}[Q_p] = \{ \mathbf{v} = [\mathbf{v}_1^T \ v_2]^T \in \mathbb{R}^4 : \mathbf{v}_1 \in \mathcal{R}^{\perp}(C), \ \mathbf{v}_1^T D(\boldsymbol{\gamma}) + v_2 \boldsymbol{\Omega}^T I_{\rm ws} = 0 \}, \tag{24}$$

which, via the fact $\mathcal{R}^{\perp}(C) = \text{span}\{\mathbf{u}\}$ leads to the condition

$$[\mathbf{u}^T \ \eta] \left[\begin{array}{c} \boldsymbol{\zeta}_1 \\ \zeta_2 \end{array} \right] = \sum_{i=1}^{N} I_{{\rm ws}i} \mathbf{u}^T \mathbf{s}_i \, \Omega_i \dot{\gamma}_i^2 - \eta \left(\sum_{i=1}^{N} I_{{\rm ws}_i} \dot{\Omega}_i^2 \right) = 0 \tag{25}$$

for all η such that $\mathbf{u}^T D(\boldsymbol{\gamma}) + \eta\, \boldsymbol{\Omega}^T I_{\mathrm{ws}} = 0$, that is, for all η such that

$$[I_{\mathrm{ws}_1} \mathbf{u}^T \mathbf{s}_1, \cdots, I_{\mathrm{ws}_N} \mathbf{u}^T \mathbf{s}_N] + \eta\, [I_{\mathrm{ws}_1} \Omega_1, \cdots, I_{\mathrm{ws}_N} \Omega_N] = 0. \tag{26}$$

If rank $M = 2$, then there does not exist an $\eta \in \mathbb{R}$ which satisfies (26), thus sufficiency follows. On the other hand, if rank $M = 1$, then there exists a nonzero scalar η satisfying (26). This yields

$$I_{\mathrm{ws}_i} \mathbf{u}^T \mathbf{s}_i = -\eta I_{\mathrm{ws}_i} \Omega_i, \qquad i = 1, \ldots, N.$$

Thus, Eq.(25) becomes

$$-\eta \left(\sum_{i=1}^{N} I_{\mathrm{ws}i} \Omega_i^2 \dot{\gamma}_i^2 + \sum_{i=1}^{N} I_{\mathrm{ws}_i} \dot{\Omega}_i^2 \right) = 0 \tag{27}$$

which cannot hold for any $[\dot{\boldsymbol{\gamma}}, \dot{\boldsymbol{\Omega}}] \neq 0$. In case $\operatorname{rank} M = 1$ it is therefore impossible to satisfy both the angular momentum (torque) and the kinetic energy (power) requirements for singularity avoidance using null motion. Therefore, the inescapable singularities of a VSCMG system used for combined attitude control and power tracking is completely characterized by the rank of the matrix M in (23). Notice that since the wheel speeds Ω_i are all positive by the definition of the spin axes $\mathbf{s}_i$, the rank deficiency of M can occur only when $\epsilon_i \triangleq \operatorname{sign}(\mathbf{u} \cdot \mathbf{s}_i) = +1$ for all $i = 1, \ldots, N$.

IV. The Angular Momentum Envelopes of a VSCMG Cluster

In this section the inescapable singularities of a VSCMG system and their relation to the rank deficiency of the matrix M in (23) are studied in more detail. For this purpose, we introduce three singular surfaces in the three-dimensional angular momentum space. The first surface is the momentum envelope for given kinetic energy, the second surface is the momentum envelope for given wheel speeds, and the third surface is the momentum envelope for given kinetic energy and gimbal angles. With the help of these three surfaces we can visualize the geometric conditions under which a singularity is either escapable or inescapable.

A. The Momentum Envelope for Given Kinetic Energy

In this section we define the angular momentum envelope of a VSCMG cluster for a given kinetic energy, and we show that the total angular momentum vector reaches this envelope if and only if the VSCMG cluster encounters an inescapable singularity (i.e., $\operatorname{rank} M{=}1$).

To this end, consider the case when a power command $P(t)$ is given for all $t_0 \leq t \leq t_f$. Then the kinetic energy stored in the VSCMG cluster for $t \geq t_0$ can be computed from $E(t) = \int_{t_0}^{t} P(t)\mathrm{d}t + E(t_0)$. Suppose that $E(\bar{t})$ is given at some instant $t = \bar{t}$. The objective is to find the maximum workspace of $\mathbf{H}(\bar{t})$ with the given value of the kinetic energy. The boundary of the maximum angular momentum workspace can be found by solving the following maximization problem.

> For a given singular direction $\mathbf{u}$, find the gimbal angles γ_i and wheel speeds Ω_i that maximize the function $\mathcal{J}$ defined by
>
> $$\mathcal{J} \triangleq \mathbf{H} \cdot \mathbf{u} = \sum_{i=1}^{N} I_{\mathrm{ws}_i} \Omega_i \mathbf{u} \cdot \mathbf{s}_i = \sum_{i=1}^{N} \alpha_i(\gamma_i) I_{\mathrm{ws}_i} \Omega_i \tag{28}$$
>
> subject to the constraints
>
> $$\sum_{i=1}^{N} I_{\mathrm{ws}_i} \Omega_i^2 = 2E \tag{29}$$
>
> $$\alpha_i^2(\gamma_i) \leq \alpha_{\max_i}^2, \quad i = 1, \ldots, N \tag{30}$$
>
> where $\alpha_i(\gamma_i) \triangleq \mathbf{u} \cdot \mathbf{s}_i$ and $\alpha_{\max_i}$ is its maximum value. Since α_i becomes maximum when $\mathbf{s}_i$ has a maximum projection onto $\mathbf{u}$ as shown in Fig. 2, $\alpha_{\max_i}$ is given by $\alpha_{\max_i} = \sqrt{1 - (\mathbf{g}_i \cdot \mathbf{u})^2}$.

In Appendix A of Ref. 6, it is shown that the solution to this maximization problem is

$$\alpha_i^* = \alpha_{\max_i}, \qquad \Omega_i^* = \frac{\alpha_{\max_i}}{2\lambda_0^*}, \qquad i = 1, \cdots, N \tag{31}$$

where

$$\lambda_0^* \triangleq \frac{1}{\sqrt{8E}} \left(\sum_{i=1}^{N} I_{\mathrm{ws}_i} \alpha_{\max_i}^2 \right)^{\frac{1}{2}}.$$

Equation (31) implies that the gimbal angles of the VSCMGs are in a singular configuration with all $\epsilon_i = +1$, and that each wheel has a speed which is proportional to $\mathbf{u} \cdot \mathbf{s}_i$. It can also be shown that the solution (31) corresponds to an inescapable singularity when $\operatorname{rank} M = 1$ (see Appendix A in Ref. 6 for the details). In summary, an inescapable singularity for the case of attitude/power tracking for a VSCMG cluster occurs when the wheels have maximum angular momentum along the singular direction with the given kinetic energy constraint.

The above observations also lend themselves to a method for drawing the angular momentum envelope of a VSCMG system with given kinetic energy constraint. Given a singular direction $\mathbf{u}$, each spin axis $\mathbf{s}_i$ is determined as in the conventional CMGs case, i.e., from Eq. (14) with all $\epsilon_i = +1$, and with the wheel speeds determined from Eq. (31). Hence, the total angular momentum at this singular configuration for a given singular direction $\mathbf{u}$ can be expressed as

$$\mathbf{H} = \sum_{i=1}^{N} \frac{(\mathbf{g}_i \times \mathbf{u}) \times \mathbf{g}_i}{\|\mathbf{g}_i \times \mathbf{u}\|} \Omega_i^* I_{\mathrm{ws}_i} = \frac{1}{2\lambda_0^*} \sum_{i=1}^{N} (\mathbf{u} - \mathbf{g}_i(\mathbf{g}_i \cdot \mathbf{u})) I_{\mathrm{ws}_i}, \tag{32}$$

where the last equality follows from $\|\mathbf{g}_i \times \mathbf{u}\| = \max\{\mathbf{s}_i \cdot \mathbf{u}\} = \alpha_{\max_i}$.

Equation (32) defines an ellipsoid in the momentum space. If the total angular momentum vector reaches this surface and the reference attitude (torque requirement) forces it outside this surface, then the VSCMG cluster cannot meet both the attitude and power tracking requirements. Contrary to the CMG case, shown in Fig. 3(a), the momentum envelope of a VSCMG cluster with given kinetic energy has no holes. The reason is that when the singular direction $\mathbf{u}$ is along a gimbal axis $\mathbf{g}_i$, the angular speed of the ith wheel does not have a component along $\mathbf{u}$ since $\mathbf{s}_i \perp \mathbf{g}_i$ and thus $\mathbf{s}_i \perp \mathbf{u}$. Hence, the ith wheel speed does not contribute to the maximization of the total angular momentum along $\mathbf{u}$. Thus, Ω_i may be taken to be zero with all the other wheels having higher speeds (in order to satisfy the kinetic energy constraint).

B. A Geometric Picture of the Inescapable Singularity Case

A nice geometric picture emerges for describing the occurrence of inescapable singularities using the previous concept of the angular momentum envelope. In addition to the angular momentum envelope for given kinetic energy introduced in the previous section, one can also define the angular momentum envelope of a VSCMG system with given energy *and* a given set of gimbal angles. Given the total kinetic energy E and the gimbal angles, this envelope is defined as the boundary of the maximum workspace of the total momentum $\mathbf{H}$ as the wheel speeds vary, but the total energy E and the gimbal angles γ_i's are kept constant. This surface can be drawn by solving the following maximization problem.

Maximize

$$\mathcal{J} \triangleq \mathbf{H} \cdot \mathbf{u} = \sum_{i=1}^{N} I_{\mathrm{ws}_i} \Omega_i \mathbf{u} \cdot \mathbf{s}_i = \sum_{i=1}^{N} \alpha_i I_{\mathrm{ws}_i} \Omega_i \tag{33}$$

subject to the constraint

$$\sum_{i=1}^{N} I_{\mathrm{ws}_i} \Omega_i^2 = 2E$$

for each $\mathbf{u} \in \mathbb{R}^3, \|\mathbf{u}\| = 1$, while the gimbal angles γ_i's are fixed.

The solution to this maximization problem is similar to the one in Section IV-A and thus, it is omitted. Its solution yields

$$\Omega_i^* = \frac{\alpha_i}{2\lambda_0^*}$$

where

$$\lambda_0^* \triangleq \frac{1}{\sqrt{8E}} \left(\sum_{i=1}^{N} I_{\mathrm{ws}_i} \alpha_i^2 \right)^{\frac{1}{2}}.$$

In addition to the angular momentum envelope for given kinetic energy and given kinetic energy and gimbal angles, one can also construct the angular momentum envelope for given wheel speeds using the method described in Section II-B. The interplay between the latter two surfaces provides a clear picture for the occurrence of the inescapable singularities.

Figures 5 and 6 show these three envelopes at a singular configuration corresponding to the singular direction $\mathbf{u} = [0, 0, 1]^T$ with $\epsilon_i > 0$ for $i = 1, 2, 3, 4$. In these figures, surface A is the momentum envelope with given wheel speeds, surface B is the momentum envelope with given energy and gimbal angles, and surface C is the momentum envelope with given kinetic energy.

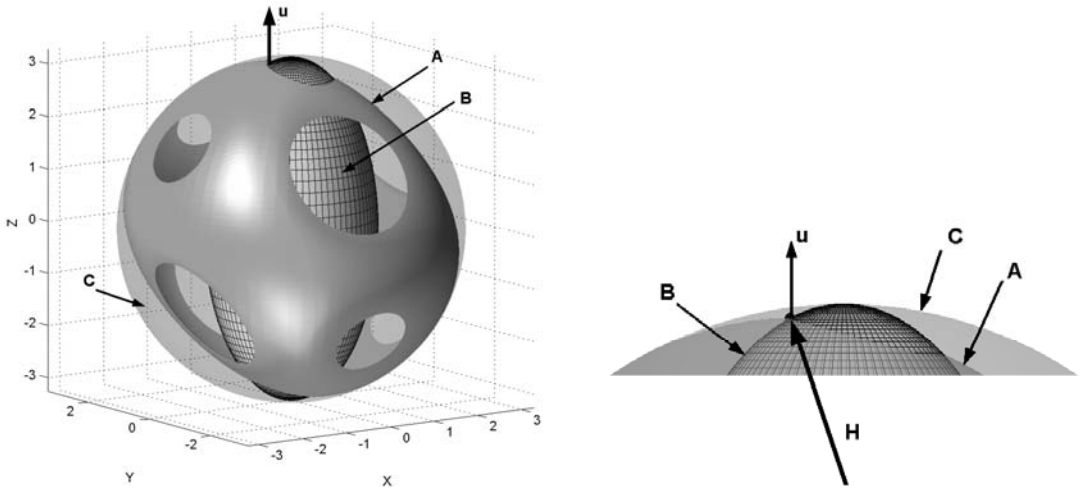

Figure 5. Escapable singularity of VSCMG

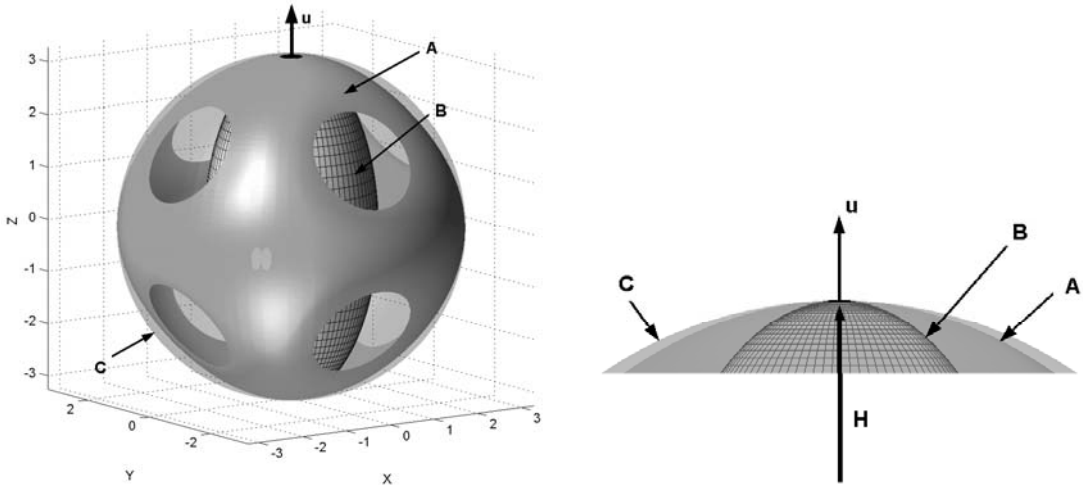

Figure 6. Inescapable singularity of VSCMG

Figure 5 shows a case when the gimbal angles are singulary configured with all $\epsilon_i > 0$, but the wheel speeds are not equal to the maximizing solution of Eq. (31) hence $\operatorname{rank} M \neq 1$. Notice that the total momentum vector $\mathbf{H}$ lies inside the momentum envelope with given energy (surface C). As the gimbal angles vary with the wheel speeds fixed, $\mathbf{H}$ will move inside the surface A, thus the projection of the change of the angular

momentum due to the gimbal changes along the singular direction is $\Delta\mathbf{H}\cdot\mathbf{u}\Big|_{\dot{\boldsymbol{\gamma}}} < 0$. As the wheel speeds vary with gimbal angles and total energy fixed, $\mathbf{H}$ will move inside the surface B, thus the projection of the change of the angular momentum due to the wheel speed changes along the singular direction, $\Delta\mathbf{H}\cdot\mathbf{u}\Big|_{\dot{\boldsymbol{\Omega}}}$, can be either positive or negative. This is shown in Fig. 5. Hence, the term $\Delta\mathbf{H}\cdot\mathbf{u}\Big|_{\dot{\boldsymbol{\Omega}}}$ can cancel the negative term $\Delta\mathbf{H}\cdot\mathbf{u}\Big|_{\dot{\boldsymbol{\gamma}}}$. Therefore, a gimbal angle change is possible without violating the angular momentum and energy constraints. As a result, in this case the singularity is escapable using null motion. On the other hand, Fig. 6 shows an inescapable singularity, i.e., when $\operatorname{rank} M = 1$. The momentum vector $\mathbf{H}$ reaches the envelope C. At this value of $\mathbf{H}$, both surface A and surface B are normal to the singular direction $\mathbf{u}$, so both $\Delta\mathbf{H}\cdot\mathbf{u}\Big|_{\dot{\boldsymbol{\gamma}}}$ and $\Delta\mathbf{H}\cdot\mathbf{u}\Big|_{\dot{\boldsymbol{\Omega}}}$ are negative. Therefore, these two cannot cancel each other. This means that gimbal angle changes and wheel speed changes while $\Delta\mathbf{H} = 0$ is impossible. Thus escaping from the singularity without violating either the momentum or the power constraints is impossible.

V. A Condition for Singularity Avoidance

If a VSCMGs cluster has a pyramid configuration with skew angle θ (see Fig. 1) and each wheel has the same moment of inertia $I_{\mathrm{w}} \triangleq I_{\mathrm{ws}_1} = I_{\mathrm{ws}_2} = I_{\mathrm{ws}_3} = I_{\mathrm{ws}_4}$, it can be shown that the momentum envelope with energy constraint E becomes an ellipsoid with the semi-axes of lengths $\sqrt{4EI_{\mathrm{w}}(1+\cos^2\theta)}$, $\sqrt{4EI_{\mathrm{w}}(1+\cos^2\theta)}$ and $\sqrt{8EI_{\mathrm{w}}}\sin\theta$ (see Appendix B in Ref. 6 for the proof of this fact). This provides a criterion for detecting whether the VSCMGs will encounter an inescapable singularity.

Theorem 1 *Consider a VSCMG cluster used for attitude and power tracking. Assume that the VSCMG cluster has a pyramid configuration with angle θ and the wheels have the same moment of inertia I_{w}. Then, for a given energy command history $E(t)$ and angular momentum command history $\mathbf{H}(t)$ for $t_0 \le t \le t_f$, the VSCMG cluster encounters an inescapable singularity, if and only if there exist $\bar{t} \in [t_0, t_f]$ such that*

$$\frac{H_x^2(\bar{t})}{4E(\bar{t})I_{\mathrm{w}}(1+\cos^2\theta)} + \frac{H_y^2(\bar{t})}{4E(\bar{t})I_{\mathrm{w}}(1+\cos^2\theta)} + \frac{H_z^2(\bar{t})}{8E(\bar{t})I_{\mathrm{w}}\sin^2\theta} \geqslant 1 \tag{34}$$

where $H_x(\bar{t}), H_y(\bar{t}), H_z(\bar{t})$ are the components of $\mathbf{H}(\bar{t})$ in the body frame.

Specifically, when the skew angle is $\theta = 54.74^\circ$, then $\cos\theta = 1/\sqrt{3}$ and $\sin\theta = \sqrt{2/3}$ and the ellipsoid becomes a sphere with radius $\sqrt{\frac{16}{3}E(\bar{t})I_{\mathrm{w}}}$. Therefore, the following is an immediate consequence of Theorem 1.

Corollary 1 *Consider a VSCMG cluster used for attitude and power tracking. Assume that the VSCMG cluster has a regular pyramid configuration (skew angle $\theta = 54.74^\circ$) and the wheels have the same moment of inertia I_{w}. Then, for a given energy command history $E(t)$ and angular momentum command history $\mathbf{H}(t)$ for $t_0 \le t \le t_f$, the VSCMG cluster encounters an inescapable singularity, if and only if there exist $\bar{t} \in [t_0, t_f]$ such that*

$$\|\mathbf{H}(\bar{t})\| \geqslant \sqrt{\frac{16}{3}E(\bar{t})I_{\mathrm{w}}}. \tag{35}$$

One method to solve the inescapable singularity problem for VSCMGs for an IPACS is therefore to increase the workspace of the VSCMGs by increasing the inertia of the wheels as suggested by (35). This means that the wheel size must be carefully determined depending on the spacecraft mission. Another possibility is to perform momentum dump/desaturation using external torque actuators such as magnetic torquers or gas thrusters. With this method, we can decrease $\|\mathbf{H}(t)\|$ thus keeping $\mathbf{H}(t)$ within the ellipsoid (or sphere) defined in Theorem 1 (or Corollary 1).

Once we know that the VSCMGs will never encounter inescapable singularities for a given attitude and power command from Theorem 1, we can apply the gradient method introduced in Ref. 11 by replacing Q with Q_p, i.e.,

$$\begin{bmatrix} \dot{\boldsymbol{\gamma}} \\ \dot{\boldsymbol{\Omega}} \end{bmatrix}_{\mathrm{null}} = -k[\mathbf{I}_{2N} - \tilde{W}^{1/2}(Q_p\tilde{W}^{1/2})^{\dagger}Q_p]\tilde{W}\begin{bmatrix} \frac{\partial\kappa}{\partial\boldsymbol{\gamma}}^T \\ \frac{\partial\kappa}{\partial\boldsymbol{\Omega}}^T \end{bmatrix} \tag{36}$$

where $A^\dagger$ denotes the Moore-Penrose inverse of the matrix A. The control law (36) will escape all singularities of the VSCMG system while tracking the required attitude and power reference commands.

VI. Numerical Examples

A numerical example is provided to test the proposed singularity avoidance method in Eq. (36). The system parameters and the reference attitude trajectory is identical with those used in Ref. 11, but in addition, the power trajectory also must be tracked in this simulation.

The results from two numerical simulations are presented below. In the first case only the attitude and power tracking control of Eq. (9) is applied. In the second case the singularity avoidance control of Eq. (36) is used simultaneously with the torque/power generating solution of (9). Figure 7 shows the reference and actual attitude histories. In these plots the subscript d designates the desired quaternion history. The spacecraft attitude tracks the desired attitude exactly after a short period of time. The reference and the actual power profiles are shown in Fig. 8. The two profiles overlap with each other perfectly and appear as a single line in Fig. 8. Figures 7 and 8 show that both attitude and power tracking are successfully achieved.

Figure 9 shows that the matrix C becomes close to being singular at approximately $t = 4000$ sec without

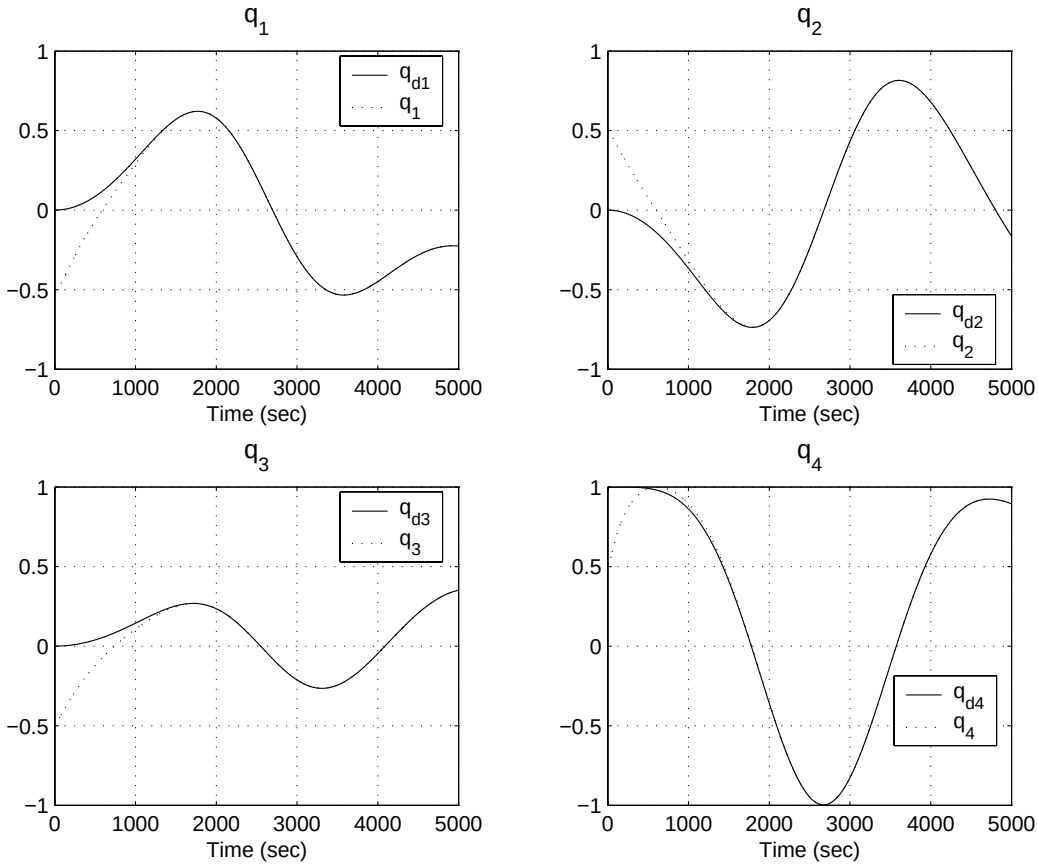

Figure 7. Reference and Actual Attitude Trajectory

any singularity avoidance algorithm. The control input $\dot{\mathbf{\Omega}}$ becomes very large during this period, since the weighting matrix W in Eq. (9) makes the VSCMGs operate in reaction wheel mode, and thus $\dot{\mathbf{\Omega}}$ has to generate the required output torque. Note that without the weighting matrix, the gimbal rate input $\dot{\boldsymbol{\gamma}}$ would become very large, instead of $\dot{\mathbf{\Omega}}$. Both cases are undesirable.

On the other hand, Fig. 10 shows that singularities are successfully avoided using the null motion algorithm of Eq. (36). Although slightly larger control inputs $\dot{\boldsymbol{\gamma}}$ are needed to reconfigure the gimbal angles as the matrix C approach the singular states, the overall magnitudes of both $\dot{\boldsymbol{\gamma}}$ and $\dot{\mathbf{\Omega}}$ are kept within a reasonable range, contrary to the case without a singularity avoidance strategy. The attitude and power

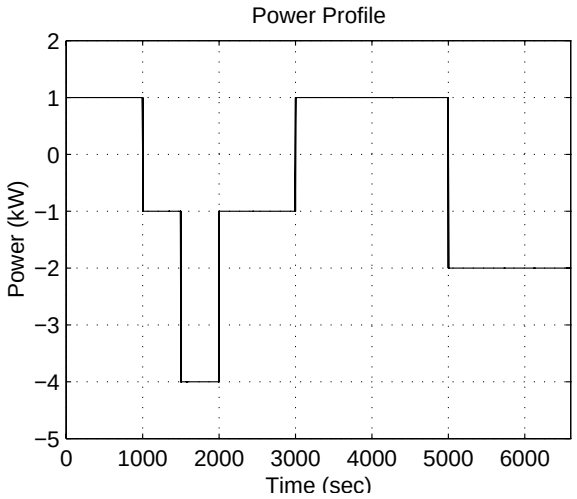

Figure 8. Desired and Actual Power Profile

history profiles are exactly the same as in the previous case and are shown in Figs. 7 and 8. It should be pointed out that the attitude and the power time histories with null motion are identical to those without null motion, that is, the null motion has affected neither the output torque nor the delivered power to the spacecraft bus, as expected.

Figure 11 shows that the singularity cannot be avoided even using the null motion method, if the criterion in Theorem 1 is violated. In Fig. 11(a), the magnitude of the total angular momentum $\|\mathbf{H}\|$ and the radius of the momentum envelope of the VSCMGs, which is equal to $\sqrt{\frac{16}{3}EI_{\mathrm{w}}}$, are plotted. During the period when $\|\mathbf{H}(t)\| < \sqrt{\frac{16}{3}E(t)I_{\mathrm{w}}}$, singularities are avoided using null motion, but when $\|\mathbf{H}(t)\| \approx \sqrt{\frac{16}{3}E(t)I_{\mathrm{w}}}$ (near $t = 6600\,\mathrm{sec}$) the condition number $\kappa(\boldsymbol{\gamma}, \boldsymbol{\Omega})$ increases, as shown in Fig. 11(b).

At this instant, the value of the matrix M defined in Eq. (23) is given by

$$M \approx \begin{bmatrix} 0.6844 & 0.6719 & 0.4073 & 0.4686 \\ \underline{0.6844} & \underline{0.6719} & \underline{0.4073} & \underline{0.4686} \\ 0.0011 & 0.0011 & 0.0011 & 0.0011 \end{bmatrix}.$$

It can be seen that at this instant the row vectors of the matrix M are parallel to each other, as expected by the analysis of Section IV.

VII. Conclusions

In this article the singularity problem associated with a VSCMGs system with a power tracking constraint is introduced and studied in detail. A VSCMG system has more degrees of freedom than a conventional CMG system, so in theory it can generate arbitrary torques. However, it cannot generate arbitrary torque and power simultaneously for some gimbal angle and wheel speed configurations.

A gradient-based method using null motion has been proposed to avoid the singularities of a VSCMG cluster, which is commanded so as to generate both attitude torque and power for an IPACS. It has been shown that the VSCMG system may encounter inescapable singularities, which cannot be avoided using the gradient method with null motion. We have shown that all such inescapable singularities are external, that is, they all lie on the momentum envelope subject to the kinetic energy constraint of the VSCMGs. Geometric and algebraic considerations provide a criterion for determining whether the VSCMGs will encounter an inescapable singularity. This criterion can be used to determine the size of a VSCMG system for a given attitude/power mission.

Acknowledgments

Support for this work has been provided through AFOSR/AFRL award F49620-00-1-0374. The authors acknowledge helpful discussions with H. Kurokawa and B. Wie concerning the CMG singularity problem.

References

[1]Tsiotras, P., Shen, H., and Hall, C., "Satellite Attitude Control and Power Tracking with Energy/Momentum Wheels," *Journal of Guidance, Control, and Dynamics*, Vol. 24, No. 1, 2001, pp. 23–34.

[2]Hall, C. D., "High-Speed Flywheels for Integrated Energy Storage and Attitude Control," *American Control Conference*, Albuquerque, NM, 1997, pp. 1894–1898.

[3]Yoon, H. and Tsiotras, P., "Spacecraft Adaptive Attitude And Power Tracking With Variable Speed Control Moment Gyroscopes," *Journal of Guidance, Control, and Dynamics*, Vol. 25, No. 6, Nov.-Dec. 2002, pp. 1081–1090.

[4]Ford, K. A. and Hall, C. D., "Flexible Spacecraft Reorientations Using Gimbaled Momentum Wheels," *Advances in the Astronautical Sciences, Astrodynamics*, edited by F. Hoots, B. Kaufman, P. J. Cefola, and D. B. Spencer, Vol. 97, Univelt, San Diego, 1997, pp. 1895–1914.

[5]Schaub, H., Vadali, S. R., and Junkins, J. L., "Feedback Control Law for Variable Speed Control Moment Gyroscopes," *Journal of the Astronautical Sciences*, Vol. 46, No. 3, 1998, pp. 307–328.

[6]Yoon, H. and Tsiotras, P., "Singularity Analysis of Variable-Speed Control Moment Gyros," *Jornal of Guidance, Control, and Dynamics*, Vol. 27, No. 3, 2004, pp. 374–386.

[7]Richie, D. J., Tsiotras, P., and Fausz, J. L., "Simultaneous Attitude Control and Energy Storage using VSCMGs : Theory and Simulation," *Proceedings of American Control Conference*, 2001, pp. 3973–3979.

[8]Schaub, H. and Junkins, J. L., "Singularity Avoidance Using Null Motion and Variable-Speed Control Moment Gyros," *Journal of Guidance Control, and Dynamics*, Vol. 23, No. 1, 2000, pp. 11–16.

[9]Wie, B., Bailey, D., and Heiberg, C. J., "Singularity Robust Steering Logic for Redundant Single-Gimbal Control Moment Gyros," *Journal of Guidance, Control, and Dynamics*, Vol. 24, No. 5, 2001, pp. 865–872.

[10]Bedrossian, N. S., Paradiso, J., Bergmann, E. V., and Rowell, D., "Steering Law Design for Redundant Single-Gimbal Control Moment Gyroscopes," *Journal of Guidance, Control, and Dynamics*, Vol. 13, No. 6, 1990, pp. 1083–1089.

[11]Yoon, H. and Tsiotras, P., "Singularity Analysis and Avoidance of Variable-Speed Control Moment Gyros – Part I : No Power Constraint Case," *Proceeding of AIAA/AAS Astrodynamics Specialist Conference and Exhibit*, Providence, Rhode Island, Aug. 2004.

[12]Kurokawa, H., "A Geometry Study of Single Gimbal Control Moment Gyros - Singularity Problem and Steering Law," Tech. Rep. Report No.175, Mechanical Engineering Laboratory, Japan, Jan. 1998.

[13]Margulies, G. and Aubrun, J. N., "Geometric Theory of Single-Gimbal Control Moment Gyro Systems," *Journal of the Astronautical Science*, Vol. 26, No. 2, 1978, pp. 159–191.

[14]Wie, B., "Singularity Analysis and Visualization for Single-Gimbal Control Moment Gyro Systems," *AIAA Guidance, Navigation, and Control Conference*, Austin, TX, August 2003, Paper No. 2003-5658.

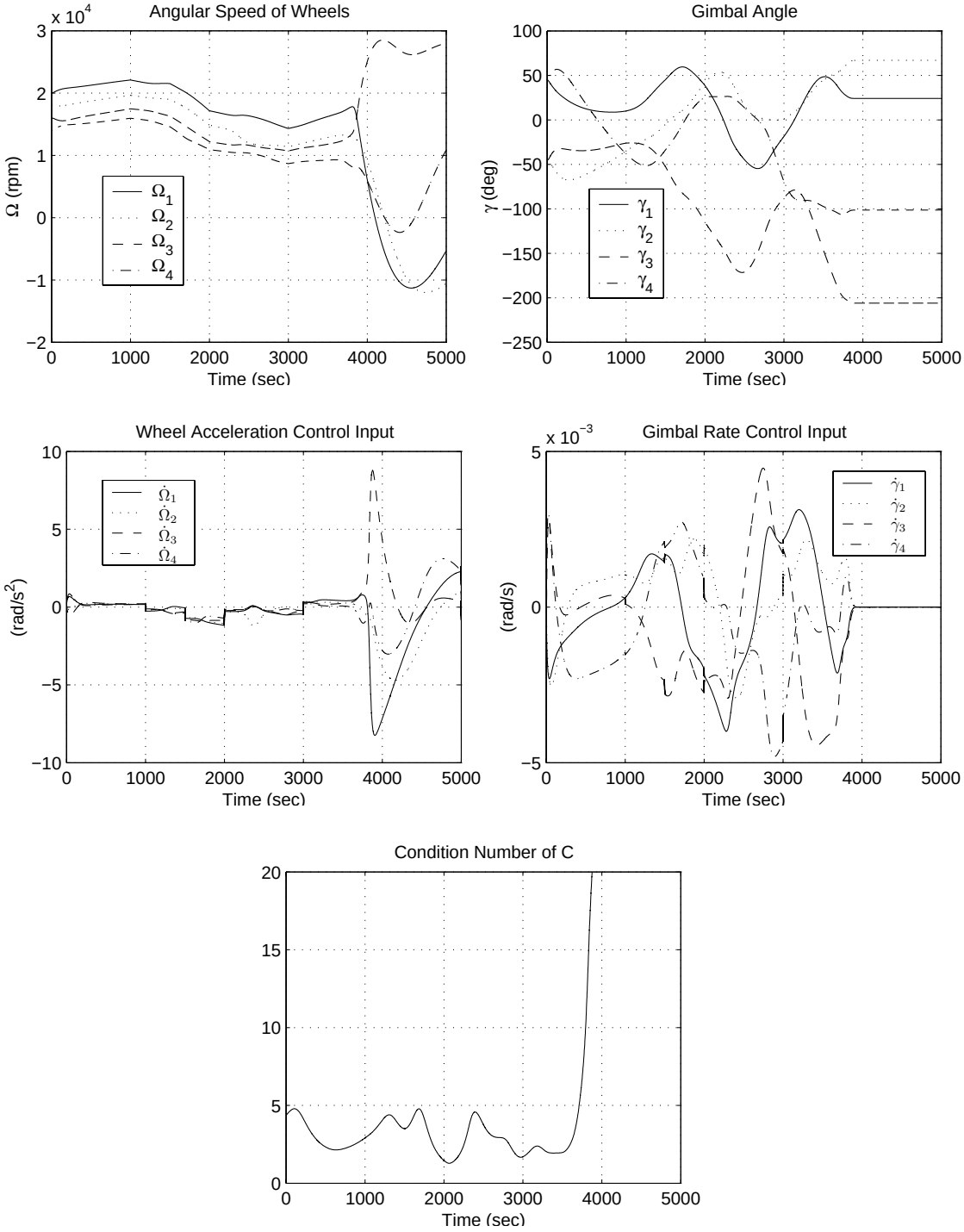

Figure 9. Simulation Without Singularity Avoidance

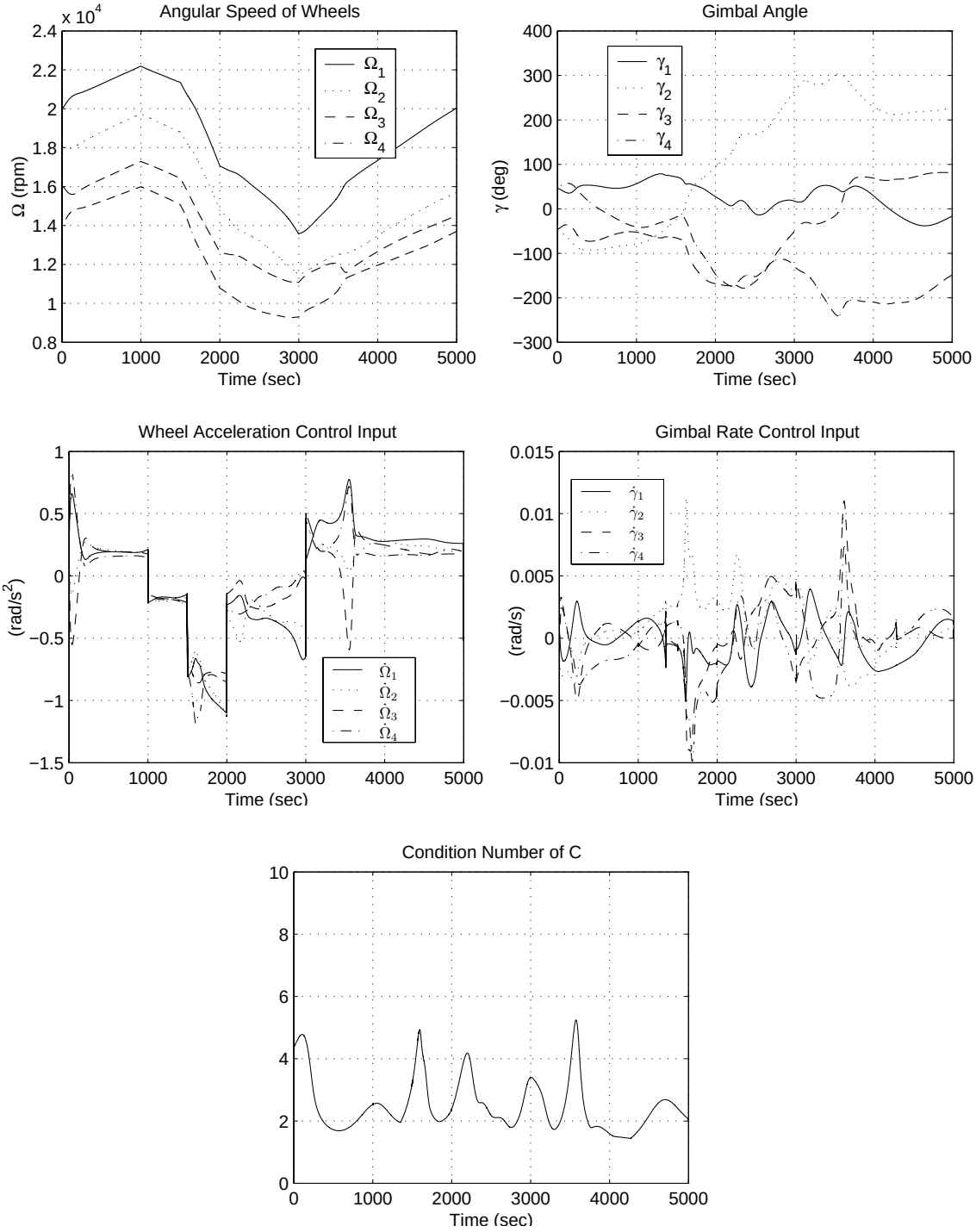

Figure 10. Simulation With Singularity Avoidance.

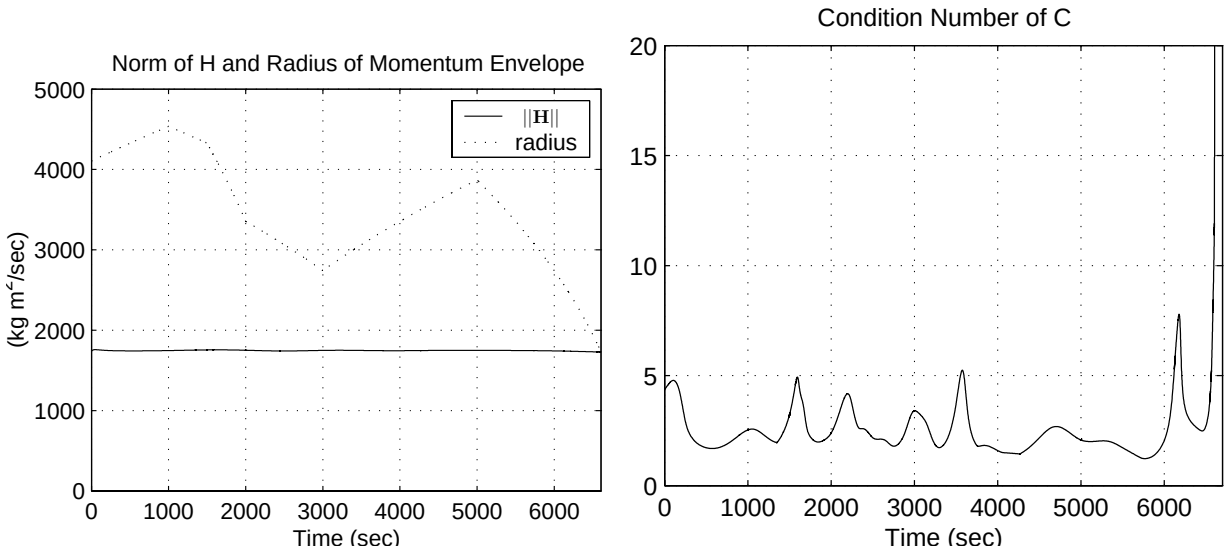

(a) Norm of $\mathbf{H}(t)$ and Radius of Momentum Envelope

(b) Condition Number of C

Figure 11. Inescapable Singularity